Title: Wave energy extraction by the end of the century: Impact of the North Atlantic Oscillation

Author(s) and affiliations: Jelena Janjić - UCD, Sarah Gallagher - Met Éireann, Emily Gleeson - Met Éireann, Frederic Dias – UCD.

Citation: Janjić J, Gallagher S, Gleeson E, Dias F. Wave Energy Extraction by the End of the Century: Impact of the North Atlantic Oscillation. ASME. International Conference on Offshore Mechanics and Arctic Engineering, *Volume 10: Ocean Renewable Energy* ():V010T09A030. doi:10.1115/OMAE2018-78107.


BY NC ND

Proceedings of
OMAE 2018
June 17-22, 2018, Madrid, Spain

OMAE2018-78107

WAVE ENERGY EXTRACTION BY THE END OF THE CENTURY: IMPACT OF THE NORTH ATLANTIC OSCILLATION

Jelena Janjić*
School of Mathematics and Statistics
University College Dublin
Dublin, Ireland
Email: jelena.janjic@ucdconnect.ie

Sarah Gallagher
Research, Environment & Applications
Met Éireann
Dublin, Ireland
Email: sarah.gallagher@met.ie

Emily Gleeson
Research, Environment & Applications
Met Éireann
Dublin, Ireland
Email: emily.gleeson@met.ie

Frédéric Dias
School of Mathematics and Statistics
University College Dublin
Dublin, Ireland
Email: frederic.dias@ucd.ie

ABSTRACT

Using wind speeds and sea ice fields from the EC-Earth global climate model to run the WAVEWATCH III model, we investigate the changes in the wave climate of the northeast Atlantic by the end of the 21^{st} *century. Changes in wave climate parameters are related to changes in wind forcing both locally and remotely. In particular, we are interested in the behavior of large-scale atmospheric oscillations and their influence on the wave climate of the North Atlantic Ocean. Knowing that the North Atlantic Oscillation (NAO) is related to large-scale atmospheric circulation, we carried out a correlation analysis of the NAO pattern using an ensemble of EC-Earth global climate simulations. These simulations include historical periods (1980–2009) and projected changes (2070–2099) by the end of the century under the RCP4.5 and RCP8.5 Representative Concentration Pathway (RCP) forcing scenarios with three members in each RCP wave model ensemble. In addition, we analysed the correlations between the NAO and a range of wave parameters that describe the wave climate from EC-Earth driven WAVEWATCH III model simulation over the North Atlantic basin, focusing on a high resolution two-way nested grid over the northeast Atlantic. The results show a distinct decrease by the end of the century and a strong positive correlation with the NAO for all wave parameters observed.*

NOMENCLATURE

F	Variance density spectrum
N	Action density spectrum
E	The first moment of the variance density spectrum
C_gE	Wave energy flux
H_s	Significant wave height
T_p	Peak period
T_{02}	Energy period

INTRODUCTION

As part of the Earth's climate system oceans are subject to climate change. The significance of the oceans in this system can be understood if we take into account that two-thirds of the Earth System is covered by water and that the heat capacity of oceans is much higher than of land. One solution to limit climate change caused by the increase in greenhouse gas concen-

*Address all correspondence to this author.

trations is to use clean energy sources e.g. ocean energy and waters of the Northeast Atlantic are ideal for ocean energy extraction. Unfortunately, climate change also has an impact on the energy resource; this needs to be investigated to provide possible solutions to changes in ocean energy extraction processes. Wave energy conversion depends on the average energy available for extraction, on extreme wave heights that may cause damage to Wave Energy Converters (WECs), and the frequency (period) of the waves because converters are most efficient when tuned to wave frequency. Changes in wave climate parameters such as wave energy flux (C_gE), wave period (T_{02} and T_p), and significant wave height (H_s) are related to changes in the wind forcing. The NAO [1] is associated with westerly winds across the North Atlantic. The amplitude and phase of the NAO are manifested in changes to the position and intensity of the Atlantic storm track [2]. The positive phase of the NAO is associated with larger waves and the negative NAO phase with smaller amplitude waves in the Northeast Atlantic. The influence of large-scale atmospheric variability on the wave climate has been extensively studied using different methodologies [3]. In the northeast Atlantic it has been shown that the NAO has a strong correlation with the wave climate of the region [4–9]. Gallagher et al. [10] showed that there is a strong correlation between station-derived NAO and H_s, wave period and peak direction for winter and spring off the west coast of Ireland using WAVEWATCH III (WW3) driven by ERA-Interim data. Gleeson et al. [11] showed a strong positive correlation between the 95th percentile of H_s and NAO, but also showed that there is a large uncertainty in the projections of higher percentiles of H_s. Decreasing trends in wind speeds and H_s have been shown in [12, 13]. We are interested in the change in the mean and 95th percentile of different wave parameters caused by the above-mentioned decreasing trend in wind speeds over the Northeast Atlantic. Though other studies may have used EC-Earth outputs to force a WW3 model (e.g. [14]), we produced a nested high resolution run of the Northeast Atlantic, which focuses with on the future of wave energy extraction.

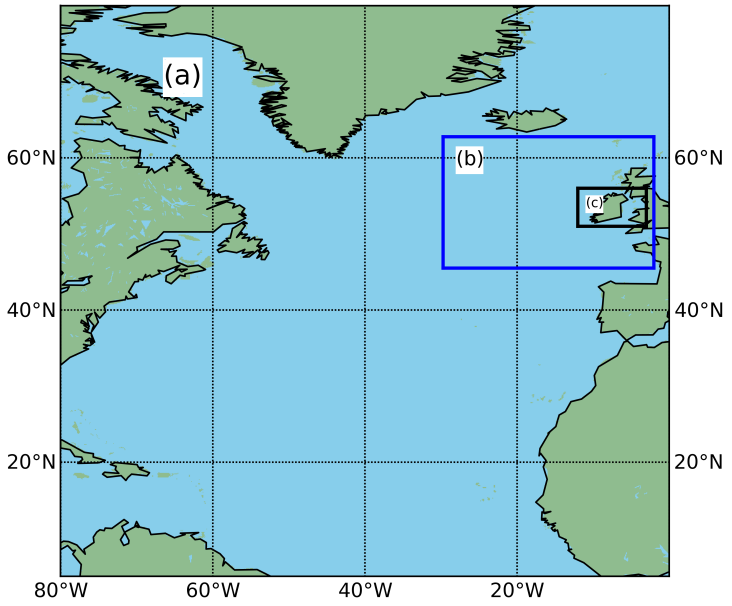

FIGURE 1. THE WAVEWATCH III MODEL DOMAINS USED IN [13]. THIS STUDY FOCUSES ON THE MIDDLE GRID B) SHOWN BY THE BLUE BOX.

MODEL DESCRIPTIONS

EC-Earth model

The EC-Earth model is one of the Earth System models [15] used in the Coupled Model Intercomparison Project Phase 5 and 6 – CMIP5 and CMIP6 [16] set up to address scientific questions that arose from the IPCC AR4 process (Intergovernmental Panel on Climate Change 4th Assessment Report) [17, 18]. Outputs of the EC-Earth model such as mean sea level pressure, wind speeds, and extratropical cyclone characteristics compared well to the European Centre for Medium-Range Weather Forecast (ECMWF) ERA-Interim reanalysis data [19]. This EC-Earth model (version 2.3) includes an atmosphere-land surface module coupled to an ocean-sea ice module [20, 21] using the the Ocean Atmosphere Sea Ice Soil coupler (OASIS) version 3 [22]. The atmospheric component of the model is based on the ECMWF Integrated Forecasting System (IFS), the oceanic component is the Nucleus for European Modelling of the Ocean version 2 (NEMO) [23] and the Sea-Ice component is the Louvain-la-Neuve Sea Ice Model (LIM) version 2 [24].

Two future scenarios or Representative Concentration Pathways (RCPs): RCP4.5 and RCP8.5 were used to run the EC-Earth model. RCP4.5 is a medium/high scenario with a radiative forcing stabilized at approximately 4.5 W/m^2 after the year 2100 and RCP8.5 is a high concentration pathway with a radiative forcing that reaches over 8.5 W/m^2 by the year 2100 [25]. Three realizations are driven by a separate EC-Earth ensemble member ($X = 1, 2, 3$) for each of the two RCP scenarios. Each wave climate ensemble member contains one historical (mei$X$) and two future simulations (me4X and me8X) corresponding to the above mentioned RCPs, producing nine 30-year data sets overall. The historical simulations were run from 1980 to 2009 and the future simulations from 2070 to 2099. In conclusion, we produced nine EC-Earth driven simulations. In addition, we ran an ERA-Interim driven hindcast (1980 to 2009) on the same model grid, used to validate the historical simulations (mei$X$, where $X = 1, 2, 3$).

WAVEWATCH III (WW3)

The WW3 model [26] solves the wave action balance equation where conservation of the action density N (the variance density F divided by the relative radian frequency σ) is balanced by source terms S that represent physical processes that generate or dissipate waves.

$$\frac{DN}{Dt} = \frac{S}{\sigma} \tag{1}$$

where

$$N = \frac{F}{\sigma} \tag{2}$$

This research studies hourly values of different wave parameters over the northeast Atlantic for the historical (1980–2009) and future (2070–2099) 30-year periods defined. The wave parameters are calculated in the WW3 model using the first moment of the variance density spectra, E, integrated over all directions (θ) and frequencies (f):

$$E = \int_0^{2\pi} \int_0^{\infty} F(f,\theta) df d\theta \tag{3}$$

This study focuses on the following wave parameters:

1. Energy flux – $C_g E$ (W/m):

$$C_g E = \rho_w g \overline{C_g} E \tag{4}$$

where $\overline{C_g}$ denotes the average group velocity over the frequency-direction spectrum (see [26]), ρ_w is the water density and g is the acceleration due to gravity.

2. Significant wave height – H_s (m):

$$H_s = 4\sqrt{E} \tag{5}$$

3. Peak period – T_p (s):

$$T_p = 1/f_p \tag{6}$$

where f_p is the peak frequency.

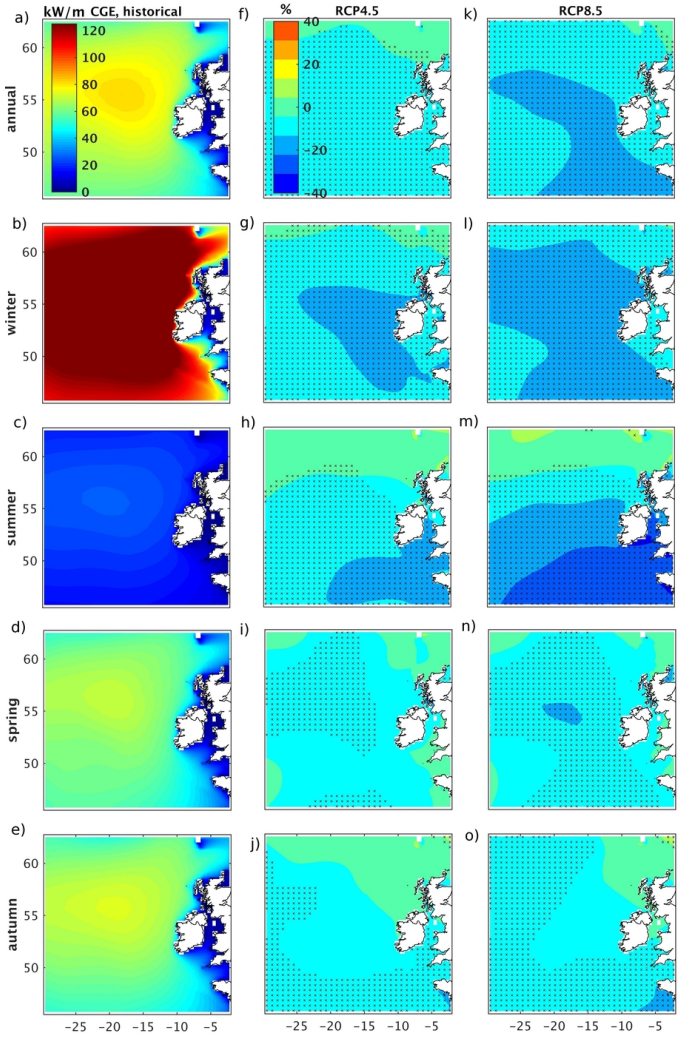

FIGURE 2. ENSEMBLE MEAN (A) ANNUAL, (B) WINTER, (C) SUMMER, (D) SPRING, AND (E) AUTUMN CGE (KW/M) FOR THE HISTORICAL PERIOD (1980–2009). PROJECTED CHANGES (%) OF CGE FOR THE PERIOD 2070–2099 RELATIVE TO 1980–2009 FOR RCP4.5 (F) ANNUAL ENSEMBLE MEAN, (G) WINTER, (H) SUMMER, (I) SPRING, (J) AUTUMN AND FOR RCP8.5 (K) ANNUAL ENSEMBLE MEAN, (L) WINTER, (M) SUMMER, (N) SPRING AND (O) AUTUMN ENSEMBLE MEAN. STIPPLING INDICATES WHERE THE % CHANGES IN THE FUTURE CGE ENSEMBLE MEAN EXCEED TWICE THE INTER-ENSEMBLE STANDARD DEVIATION.

4. Zero-upcrossing wave period – T_{02} (s):

$$T_{02} = \frac{2\pi}{\sqrt{\sigma^2}} \tag{7}$$

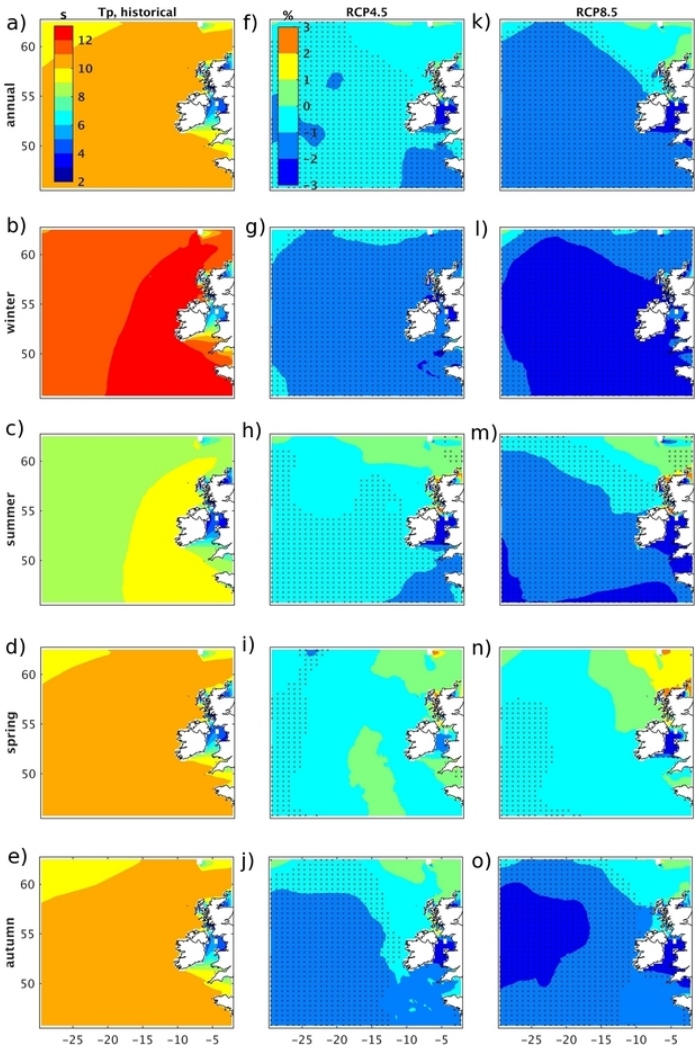

FIGURE 3. ENSEMBLE MEAN (A) ANNUAL, (B) WINTER, (C) SUMMER, (D) SPRING, AND (E) AUTUMN T_p (s) FOR THE HISTORICAL PERIOD (1980–2009). PROJECTED CHANGES (%) OF T_p FOR THE PERIOD 2070–2099 RELATIVE TO 1980– 2009 FOR RCP4.5 (F) ANNUAL ENSEMBLE MEAN, (G) WINTER, (H) SUMMER, (I) SPRING, (J) AUTUMN AND FOR RCP8.5 (K) ANNUAL ENSEMBLE MEAN, (L) WINTER, (M) SUMMER, (N) SPRING AND (O) AUTUMN ENSEMBLE MEAN. STIPPLING INDICATES WHERE THE % CHANGES IN THE FUTURE T_p ENSEMBLE MEAN EXCEED TWICE THE INTER-ENSEMBLE STANDARD DEVIATION.

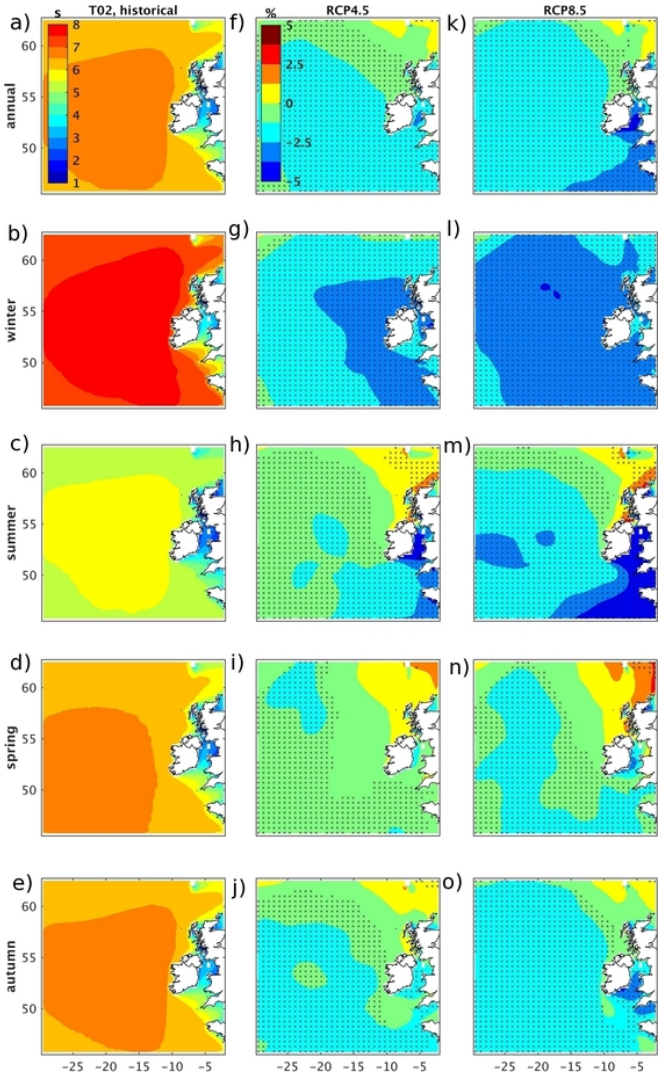

FIGURE 4. ENSEMBLE MEAN (A) ANNUAL, (B) WINTER, (C) SUMMER, (D) SPRING, AND (E) AUTUMN T_{02} (s) FOR THE HISTORICAL PERIOD (1980–2009). PROJECTED CHANGES (%) OF T_{02} FOR THE PERIOD 2070–2099 RELATIVE TO 1980– 2009 FOR RCP4.5 (F) ANNUAL ENSEMBLE MEAN, (G) WINTER, (H) SUMMER, (I) SPRING, (J) AUTUMN AND FOR RCP8.5 (K) ANNUAL ENSEMBLE MEAN, (L) WINTER, (M) SUMMER, (N) SPRING AND (O) AUTUMN ENSEMBLE MEAN. STIPPLING INDICATES WHERE THE % CHANGES IN THE FUTURE T_{02} ENSEMBLE MEAN EXCEED TWICE THE INTER-ENSEMBLE STANDARD DEVIATION.

where σ is n intrinsic radian frequency (for more details see [26]).

EC-Earth 10 m wind speeds and sea ice fields and ERA-Interim data were used to force the model. The model uses three two-way nested grids (see Fig. 1). The grid (a) covers the North Atlantic, grid (b) covers a large area of the northeast Atlantic, and the grid around Ireland (c) is an unstructured grid with a varying resolution. The reason behind using the middle grid (b) instead of the higher resolution grid (c) is that (b) covers the Northeast

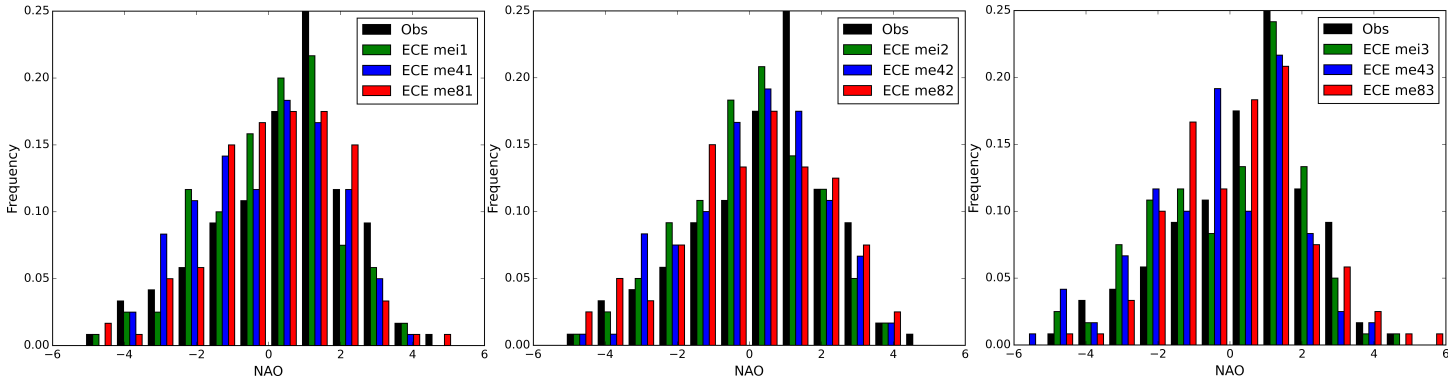

FIGURE 5. HISTOGRAM OF THE NAO INDEX FOR: (LEFT) OBSERVATIONS (1980–2009) IN BLACK, EC-EARTH mei1 (1980–2009) IN GREEN, EC-EARTH me41 (2070–2099) IN BLUE, AND EC-EARTH me81 (2070–2099) IN RED; (MIDDLE) SHOWS THE SAME FOR ENSEMBLE NUMBER 2; (RIGHT) SHOWS THE SAME FOR ENSEMBLE NUMBER 3.

Atlantic ($0.25^\circ \times 0.25^\circ$ resolution), as opposed to the grid around the nearshore of Ireland, which was examined in [13] and [27]. This provides an opportunity to examine the west coast of Scotland and France as well as Ireland, which are areas with high wave energy potential.

METHODOLOGY

The EC-Earth model was used to produce the atmospheric datasets, the WW3 model was used to generate the wave datasets and we used the National Centre for Atmospheric Research (NCAR) NAO station-base time-series.

The NAO index (an indicator of North Atlantic Oscillation phase and strength) depends on the method used in its definition. We used the monthly observation station-based NAO index by NCAR which was computed using the values of MSLP (Mean Sea Level Pressure) recorded in Reykjavik (Iceland) and Ponta Delgada (Azores) [28]. For each month the raw data for each station is normalised separately by the 1864–1983 long term means. Finally, the NAO station index is the difference between the Reykjavik and Ponta Delgado normalised values. EC-Earth MSLP values were extracted using the nearest neighbour remapping algorithm (remapnn) available in the CDO (Climate Data Operators) package [29]. Finally, the National Centre for Atmospheric Research (NCAR) NAO station-base time-series were compared to the NAO index computed using EC-Earth MSLP values to determine the ability of the EC-Earth model to simulate the NAO.

We performed a correlation analysis that measures the strengths of association between two variables (the NAO and the chosen wave parameter) and the direction of the relationship. The value of the correlation coefficient varies between +1 and -1. A value of the correlation coefficient close to $\pm$ 1 represents an almost perfect degree of association between the two variables; in the case of a value being close to 0 the relationship between the variables is weak. A positive correlation coefficient means that the variables change in phase and if the correlation coefficient is negative the variables change in the opposite direction. Usually, in statistics, there are four definitions of correlation: Pearson correlation, Kendall rank correlation, Spearman correlation, and the Point-Biserial correlation. The Spearman correlation coefficient, which expresses the statistical non-parametric measure of the strength of a monotonic relationship between paired data, was used in this study.

This study is an extension of the work done in [30]. We have added a detailed analysis of the NAO correlation to four different wave parameters and looked at two different wave periods, their correlation to NAO and expected changes by the end of the 21st century.

VALIDATION

In order to validate the ability of the EC-Earth model to simulate the change in the NAO index we have compared the observed NAO index to the historical and future values of the NAO index computed using all three EC-EARTH ensemble members (see Fig. 5). Comparing the historical EC-Earth NAO index and the observations we can see that there is a good agreement. Furthermore, if we take a look at the predicted future NAO index we see there are no drastic changes by the end of the 21st century. The EC-Earth forced WW3 model outputs were compared to the ERA-Interim hindcast showing just a 5% difference off the west coast of Ireland. The ERA-Interim driven WW3 run was compared to buoy measurements and showed good correlation. More details on the validation of the analysed wave dataset can be found in [13, 31, 32].

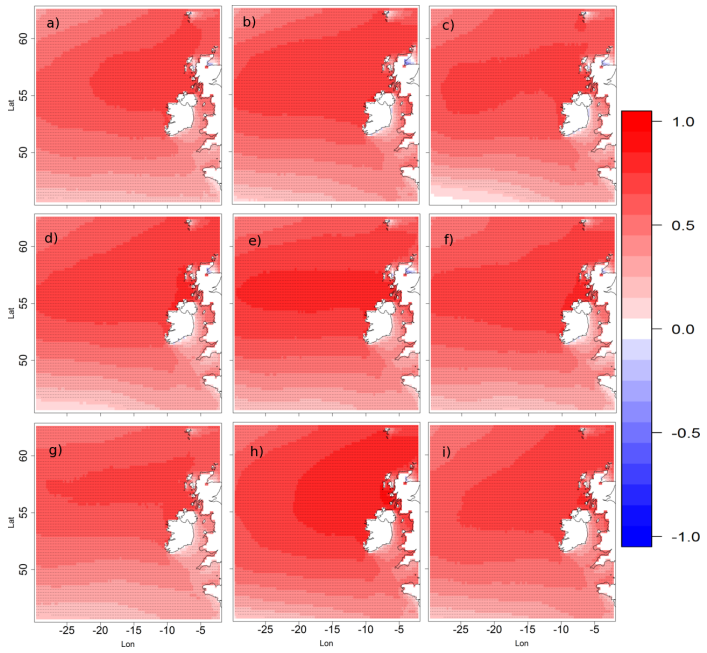

FIGURE 6. THE SPEARMAN CORRELATION COEFFICIENT BETWEEN THE NAO INDEX AND THE MEAN WAVE ENERGY FLUX (C_gE) FOR DJFM (DJFM = DECEMBER, JANUARY, FEBRUARY, AND MARCH). (A–C) HISTORICAL PERIOD (1980–2009) 3 $\times$ ENSEMBLE MEMBERS (MEI1, MEI2, AND MEI3); (D–F) FUTURE PERIOD 2070–2099 UNDER RCP4.5 (ME41, ME42, AND ME43) AND SIMILARLY (G–I) IS FOR 2070–2099 UNDER RCP8.5 (ME81, ME82, AND ME83). CORRELATIONS STATISTICALLY SIGNIFICANT AT THE $\alpha < 0.05$ LEVEL ARE DOTTED.

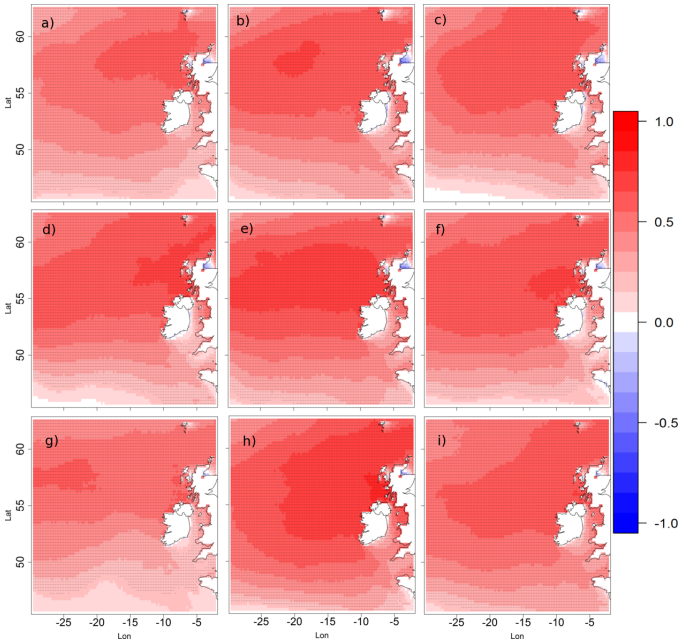

FIGURE 7. THE SPEARMAN CORRELATION COEFFICIENT BETWEEN THE NAO INDEX AND THE 95TH PERCENTILE OF THE WAVE ENERGY FLUX (C_gE) FOR DJFM (DJFM = DECEMBER, JANUARY, FEBRUARY, AND MARCH). (A–C) HISTORICAL PERIOD (1980–2009) 3 $\times$ ENSEMBLE MEMBERS (MEI1, MEI2, AND MEI3); (D–F) FUTURE PERIOD 2070–2099 UNDER RCP4.5 (ME41, ME42, AND ME43) AND SIMILARLY (G–I) IS FOR 2070–2099 UNDER RCP8.5 (ME81, ME82, AND ME83). CORRELATIONS STATISTICALLY SIGNIFICANT AT THE $\alpha < 0.05$ LEVEL ARE DOTTED.

RESULTS

The first column of Fig. 2 shows the annual and seasonal ensemble mean wave energy flux C_gE for the historical period (1980–2009). The second and third columns represent the percentage differences between the historical and future ensemble means under RCP4.5 and RCP8.5 respectively. Figures 3 and 4 have the same layout as Fig. 2 but show T_p and T_{02}. The annual value of the wave energy flux ranges from 60 to 80 kW/m for the historical period. As expected, the wave energy is largest in winter and smallest in summer. The ensemble means spring and autumn have similar values. In the winter the wave energy flux reaches a value of 120 kW/m, while during the summer it does not exceed 40 kW/m. Since cooler tones represent a decrease, we can see that the decrease is present in all seasons and annually for both future scenarios with the summer under RCP8.5 having the largest relative decrease of around 30%. The absolute decrease for winter reaches 30 kW/m for both scenarios. The annual decrease is around 10% under RCP4.5 to 20% under RCP8.5. There are areas of increase but these are not statistically significant. Changes by the end of the century in spring and autumn are statistically insignificant over which half of the area of interest.

T_p represents the period of strongest waves in the spectrum of waves over the observed area. The annual peak period is mostly 10 to 11 seconds. Again, the longest wave periods occur in winter (11–13 seconds) off the west coast of Ireland, the shortest in the summer (8–10 seconds) for the historical ensemble mean. This coincides with the fact that the most energetic waves are waves with the longest wave periods. During summer and autumn the value of T_p ranges from 9 to 11 seconds. Looking at the second and third columns of Fig. 3 we can see both annual and seasonal decrease for both future scenarios compared to 1980–2009. The annual decrease of this wave parameter ranges from 1.25% to 2.5% under RCP4.5 and 3.75% for the southeast of the area under RCP8.5. There is a relative decrease of 2.5% to 3.75% over a large area for winter and autumn under RCP8.5. There is also a large area showing a decrease in T_p between 3.75% and 5% in autumn under RCP8.5. In comparison to Fig.2 we see that the changes by the end of the 21st century

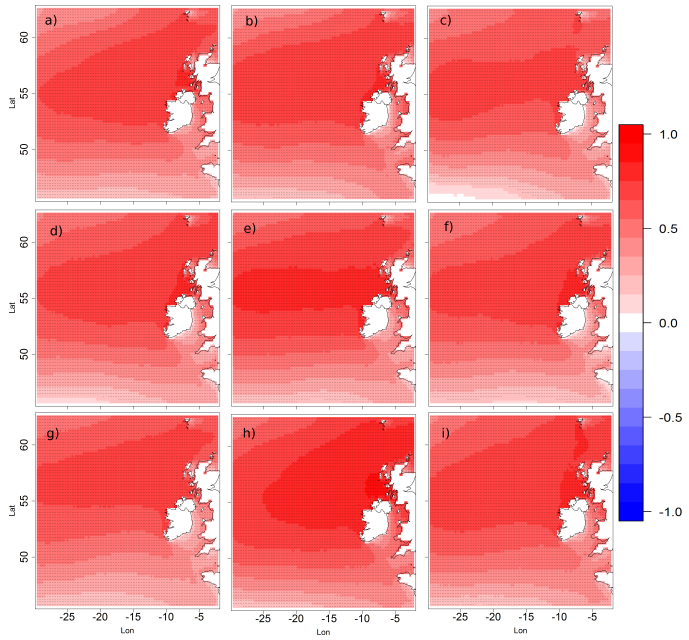

FIGURE 8. THE SPEARMAN CORRELATION COEFFICIENT BETWEEN THE NAO INDEX AND THE MEAN SIGNIFICANT WAVE HEIGHT (H_s) FOR DJFM (DJFM = DECEMBER, JANUARY, FEBRUARY, AND MARCH). (A–C) HISTORICAL PERIOD (1980–2009) 3 $\times$ ENSEMBLE MEMBERS (MEI1, MEI2, AND MEI3); (D–F) FUTURE PERIOD 2070–2099 UNDER RCP4.5 (ME41, ME42, AND ME43) AND SIMILARLY (G–I) IS FOR 2070–2099 UNDER RCP8.5 (ME81, ME82, AND ME83). CORRELATIONS STATISTICALLY SIGNIFICANT AT THE $\alpha < 0.05$ LEVEL ARE DOTTED.

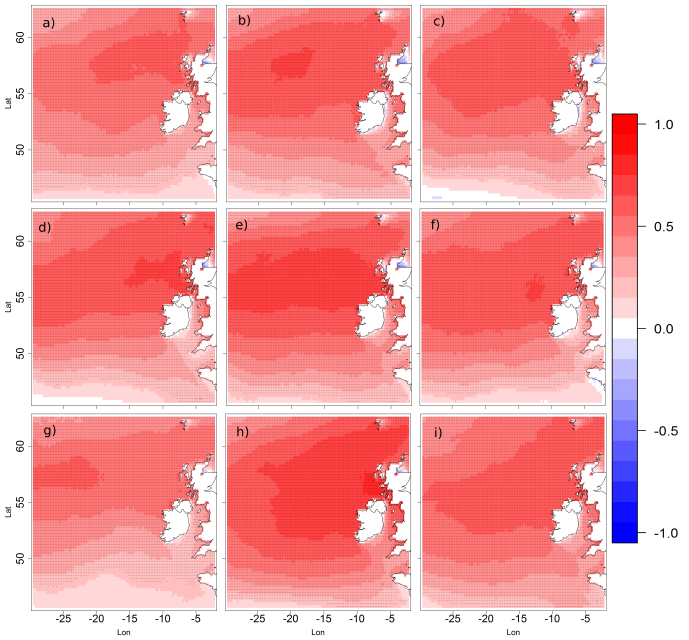

FIGURE 9. THE SPEARMAN CORRELATION COEFFICIENT BETWEEN THE NAO INDEX AND THE 95TH PERCENTILE OF THE SIGNIFICANT WAVE HEIGHT (H_s) FOR DJFM (DJFM = DECEMBER, JANUARY, FEBRUARY, AND MARCH). (A–C) HISTORICAL PERIOD (1980–2009) 3 $\times$ ENSEMBLE MEMBERS (MEI1, MEI2, AND MEI3); (D–F) FUTURE PERIOD 2070–2099 UNDER RCP4.5 (ME41, ME42, AND ME43) AND SIMILARLY (G–I) IS FOR 2070–2099 UNDER RCP8.5 (ME81, ME82, AND ME83). CORRELATIONS STATISTICALLY SIGNIFICANT AT THE $\alpha < 0.05$ LEVEL ARE DOTTED.

for T_p are less spatially homogeneous than for C_gE and the spring differences under RCP4.5 and RCP8.5 are mostly statistically insignificant.

The zero-upcrossing period T_{02} or the mean wave period shown in Fig. 4. The annual value of the historical ensemble mean is 6 to 7 s. The mean for the historical ensemble for the winter period shows a value for T_{02} of up to 8 seconds while the summer values range from 5 to 6 s. The autumn and spring means range from 6 to 7 seconds. Once more the future changes of this parameter are less spatially homogeneous than the wave energy flux but there is still a decrease annually and seasonally under both RCPs. The annual change in T_{02} by the end of the 21st century is mostly a decrease from 1.25% to 2.5% under RCP4.5 and 3.75% under RCP8.5 in the southeast. The future changes in T_{02} are statistically insignificant in large areas especially under RCP4.5. The most significant relative decrease is found in the southeast of the area of interest (3.75% to 5% in summer and a large area of decrease from 2.5% to 3.75% in the winter). The areas of increase are statistically insignificant, except for small area in the northeast in summer. Annually, large areas are predicted to experience a decrease from 1.25% to 2.5%.

The mean and 95th percentile values of above mentioned parameters (C_gE, H_s, T_{02}, and T_p) were correlated with the NAO index in Fig. 6, 7, 8, 9, 10, and 11. The first row of these figures represents the three historical (1980–2009) ensemble members (mei1, mei2, and mei3), the second shows the future (2070–2099) RCP4.5 ensemble members (me42, me42, and me43), and finally the third row shows for the future (2070–2099) RCP8.5 ensemble members (me81, me82, and me83).

The mean wave energy off the west coast of Ireland is strongly positively correlated to the NAO index for the historical and future periods for each ensemble member with maximum values of between 0.7 and 0.9 (Fig.6). There is a slightly stronger correlation over larger areas for me42 and me82 of over 0.8 (subplots e and h) than for the historical or other future ensemble members. The NAO index and the 95th percentile of C_gE are slightly less correlated than the mean C_gE with the NAO index, but there is a strong positive correlation off the west coast of Ireland (Fig. 7) with maxima ranging from 0.6 to 0.8. The

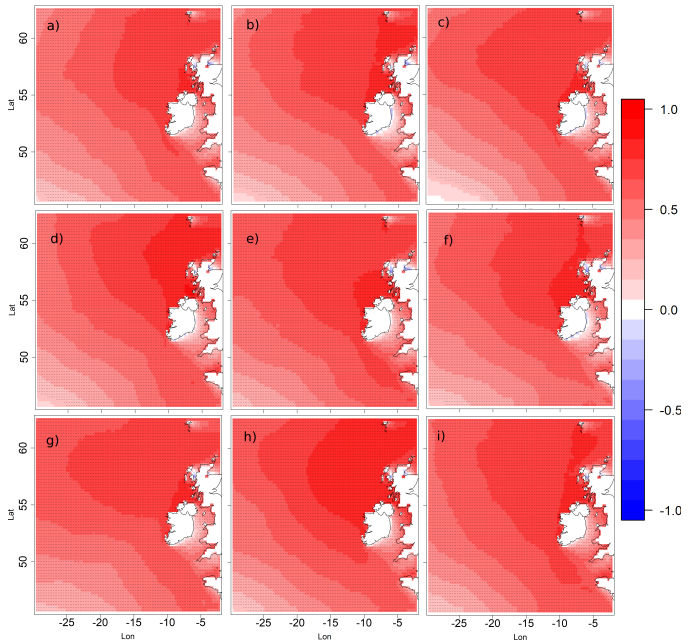

FIGURE 10. THE SPEARMAN CORRELATION COEFFICIENT BETWEEN THE NAO INDEX AND THE MEAN ZERO-UPCROSSING PERIOD (T_{02}) FOR DJFM (DJFM = DECEMBER, JANUARY, FEBRUARY, AND MARCH). (A–C) HISTORICAL PERIOD (1980–2009) 3 × ENSEMBLE MEMBERS (MEI1, MEI2, AND MEI3); (D–F) FUTURE PERIOD 2070–2099 UNDER RCP4.5 (ME41, ME42, AND ME43) AND SIMILARLY (G–I) IS FOR 2070–2099 UNDER RCP8.5 (ME81, ME82, AND ME83). CORRELATIONS STATISTICALLY SIGNIFICANT AT THE $\alpha < 0.05$ LEVEL ARE DOTTED.

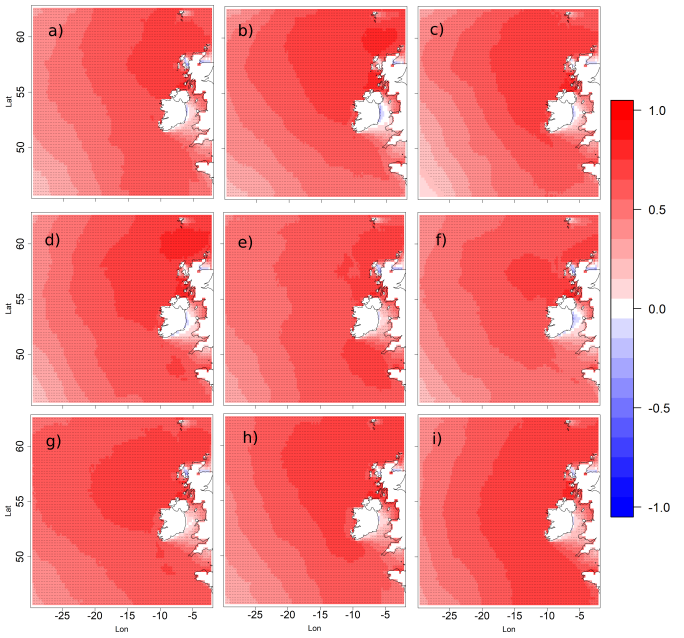

FIGURE 11. THE SPEARMAN CORRELATION COEFFICIENT BETWEEN THE NAO INDEX AND THE MEAN PEAK PERIOD (T_p) FOR DJFM (DJFM = DECEMBER, JANUARY, FEBRUARY, AND MARCH). (A–C) HISTORICAL PERIOD (1980–2009) 3 × ENSEMBLE MEMBERS (MEI1, MEI2, AND MEI3); (D–F) FUTURE PERIOD 2070–2099 UNDER RCP4.5 (ME41, ME42, AND ME43) AND SIMILARLY (G–I) IS FOR 2070–2099 UNDER RCP8.5 (ME81, ME82, AND ME83). CORRELATIONS STATISTICALLY SIGNIFICANT AT THE $\alpha < 0.05$ LEVEL ARE DOTTED.

pattern of correlation for both mean and 95th percentile of C_gE is orientated west-east.

The Fig. 9 is presented in [11]. There is a very strong correlation between the mean H_s and the NAO index with maxima ranging from 0.75 to 0.9 for both historical and future ensemble members. A strong correlation coefficient over a significant portion of the area can be seen in subplots e and h (me42 and me82). There is a weaker correlation between the 95th percentile of H_s and the NAO than for the mean values of H_s, with maxima ranging from 0.6 to 0.7 for all future and past ensemble members except me42 and me82 (over 0.7) and me81 (less than 0.6). The pattern of correlation for both the mean and 95th percentile of H_s is predominantly orientated in a west-east direction.

Fig. 10 shows a strong positive correlation between T_{02} and the NAO for both the historical and future periods and all ensemble members with maximum values ranging mostly from 0.8 to 0.9. me82 shows a stronger correlation over a larger area than other subplots in Fig.10. It is interesting to note that the pattern of correlation is oriented in the northeast-southwest direction. This might be due to the position of the northeast Atlantic mid-latitude storm track. For the mean peak period (Fig.11) there are maximum values of the correlation coefficient ranging from approximately 0.75 to 0.85. The highest correlation coefficient is for mei2 (0.83) and the lowest for me81 (0.76). The orientation of the correlation pattern is in the northeast-southwest direction. Comparing T_{02} and T_p we can see that the correlation is slightly higher and more spatially homogeneous for T_{02} than T_p. The reason behind this could be that T_{02} is a mean period while T_p is the period of the highest waves and we have already observed that the means correlate better with the NAO than extremes.

CONCLUSIONS

This study used EC-EARTH model fields (sea ice and 10 m winds) to force a nested WAVEWATCH III model. Following the model validation, four wave parameters, important for wave energy conversion – C_gE, H_s, T_{02}, and T_p were analysed. Energy available for extraction (C_gE), the height of 1/3 of the highest waves (H_s) and the frequency/period at which waves propagate

(T_{02} and T_p) are important for the process of wave energy extraction. Therefore, by analysing these parameters we see that there is a statistically significant decrease expected in the wave energy flux by the end of the century of up to 30 kW/m. The longest period waves are the most energetic, therefore, we might have expected the decrease in the wave periods (T_{02} and T_p). Though the decrease in the periods is not spatially homogeneous for each future ensemble mean and in some seasons not statistically significant, we still have a predicted decrease ranging from 1% to 5% for T_{02} and T_p. Accordingly, certain steps need to be taken in the future so that changes in the wave climate do not interfere with the efficiency of the wave energy extraction processes.

The correlation between the NAO index and the wave parameters is strongly positive, stronger for the mean values of the parameters than their 95th percentiles. The maximum values of the correlation coefficient between the mean values of the wave parameters and the NAO index range between 0.7 and 0.9 and for the 95th percentile mostly between 0.5 and 0.8. It is interesting to note that the pattern of correlation for the significant wave height and wave energy flux is oriented west-east but southwest-northeast for the wave periods.

ACKNOWLEDGMENT

This work is supported by Science Foundation Ireland (SFI) through Marine Renewable Energy Ireland (MaREI), the SFI Centre for Marine Renewable Energy Research-(12/RC/2302). The authors acknowledge Roxana Tiron who helped run the simulations and the Irish Centre for High-End Computing (ICHEC) for the provision of computational facilities.

REFERENCES

[1] Barnston, A. G., and Livezey, R. E., 1987. "Classification, Seasonality and Persistence of Low-Frequency Atmospheric Circulation Patterns". *Monthly Weather Review,* ***115***(6), pp. 1083–1126.

[2] Scherrer, S. C., Croci-Maspoli, M., Schwierz, C., and Appenzeller, C., 2006. "Two-dimensional indices of atmospheric blocking and their statistical relationship with winter climate patterns in the Euro-Atlantic region". *International Journal of Climatology,* ***26***(2), pp. 233–249.

[3] Martínez-Asensio, A., Tsimplis, M. N., Marcos, M., Feng, X., Gomis, D., Jordá, G., and Josey, S. A., 2016. "Response of the North Atlantic wave climate to atmospheric modes of variability". *International Journal of Climatology,* ***36***(3), pp. 1210–1225.

[4] Atan, R., Goggins, J., and Nash, S., 2016. "A detailed assessment of the wave energy resource at the Atlantic Marine Energy Test Site". *Energies,* ***9***(11), pp. 1996–1073.

[5] Bertin, X., Prouteau, E., and Letetrel, C., 2013. "A significant increase in wave height in the North Atlantic ocean over the 20th century". *Global and Planetary Change,* ***106***(Supplement C), pp. 77–83.

[6] Charles, E., Idier, D., Thiébot, J., Le Cozannet, G., Pedreros, R., Ardhuin, F., and Planton, S., 2012. "Present wave climate in the Bay of Biscay: spatiotemporal variability and trends from 1958 to 2001". *Journal of Climate,* ***25***(6), pp. 2020–2039.

[7] Dodet, G., Bertin, X., and Taborda, R., 2010. "Wave climate variability in the North-East Atlantic Ocean over the last six decades". *Ocean Modelling,* ***31***(3), pp. 120–131.

[8] Le Cozannet, G., Lecacheux, S., Delvallee, E., Desramaut, N., Oliveros, C., and Pedreros, R., 2011. "Teleconnection pattern influence on sea-wave climate in the Bay of Biscay". *Journal of Climate,* ***24***(3), pp. 641–652.

[9] Santo, H., Taylor, P., and Gibson, R., 2016. "Decadal variability of extreme wave height representing storm severity in the northeast Atlantic and North Sea since the foundation of the Royal Society". In Proceedings of the Royal Society of London A: Mathematical, Physical and Engineering Sciences, Vol. 472, The Royal Society.

[10] Gallagher, S., Tiron, R., and Dias, F., 2014. "A Long-Term Nearshore Wave Hindcast for Ireland: Atlantic and Irish Sea coasts (1979–2012)". *Ocean Dynamics,* ***64***(8), pp. 1163–1180.

[11] Gleeson, E., Gallagher, S., Clancy, C., and Dias, F., 2017. "NAO and Extreme Ocean States in the Northeast Atlantic Ocean". *Advances in Science and Research,* ***14***, pp. 23–33.

[12] Dobrynin, M., Murawsky, J., and Yang, S., 2012. "Evolution of the Global Wind Wave Climate in CMIP5 Experiments". *Geophysical Research Letters,* ***39***(18).

[13] Gallagher, Sarah and Gleeson, Emily and Tiron, Roxana and McGrath, Ray and Dias, Frédéric, 2016. "Wave Climate Projections for Ireland for the End of the 21st Century Including Analysis of EC-Earth winds over the North Atlantic Ocean". *International Journal of Climatology,* ***36***(14), pp. 4592–4607.

[14] Casas-Prat, M., Wang, X., and Swart, N., 2018. "CMIP5-based global wave climate projections including the entire Arctic Ocean". *Ocean Modelling,* ***123***, pp. 66–85. ISSN 1463-5003.

[15] Wang, X. L., Feng, Y., and Swail, V. R., 2015. "Climate change signal and uncertainty in projections of ocean wave heights". *Journal of Geophysical Research: Oceans,* ***120***(5), pp. 3859–3871.

[16] Taylor, K. E., Stouffer, R. J., and Meehl, G. A., 2012. "An Overview of CMIP5 and the Experiment Design". *Journal of Geophysical Research: Oceans,* ***93***(4), pp. 485–498.

[17] Solomon, S., 2007. *Climate change 2007 – The physical science basis: Working group I contribution to the fourth assessment report of the IPCC (Vol. 4)*. Cambridge University Press, Cambridge, United Kingdom.

[18] van der Linden, P. J., and Hanson, C. E., 2007. *Climate change 2007 − Impacts, adaptation and vulnerability: Working group II contribution to the fourth assessment report of the IPCC (Vol. 4)*. Cambridge University Press, Cambridge, United Kingdom.

[19] Dee, D. P., Uppala, S. M., Simmons, A. J., Berrisford, P., Poli, P., Kobayashi, S., Andrae, U., Balmaseda, M. A., Balsamo, G., Bauer, P., and et al., 2011. "The ERA-Interim Reanalysis: Configuration and Performance of the Data Assimilation System". *Quarterly Journal of the Royal Meteorological Society,* ***137***(656), pp. 553–597.

[20] Hazeleger, W., Wang, X., Severijns, C., Ştefănescu, S., Bintanja, R., Sterl, A., Wyser, K., Semmler, T., Yang, S., van den Hurk, B., van Noije, T., van der Linden, E., and van der Wiel, K., 2012. "EC-Earth V2.2: Description and Validation of a New Seamless Earth System Prediction Model". *Climate Dynamics,* ***39***(11), pp. 2611–2629.

[21] Hazeleger, W., Severijns, C., Semmler, T., Ştefănescu, S., Yang, S., Wang, X., Wyser, K., Dutra, E., Baldasano, J., Bintanja, R., et al., 2010. "EC-Earth V2.2: Description and Validation of a New Seamless Earth System Prediction Model". *Bulletin of the American Meteorological Society,* ***91***(10), pp. 1357–1363.

[22] Valcke, S., 2006. *OASIS3 User Guide (prism_2-5) Support Initiative Report No 3*. CERFACS. See also URL http://www.cerfacs.fr/oa4web/papers_oasis/oasis3_UserGuide.pdf.

[23] Madec, G., and Institut Pierre-Simon Laplace, 2008. "NEMO Ocean Engine, Note du Pôle de Modélisation, 27".

[24] Fichefet, T., and Maqueda, M. A. M., 1997. "Sensitivity of a Global Sea Ice Model to the Treatment of Ice Thermodynamics and Dynamics". *Journal of Geophysical Research: Oceans,* ***102***(C6), pp. 12609–12646.

[25] Moss, R., Babiker, W., Brinkman, S., Calvo, E., Carter, T., Edmonds, J., Elgizouli, I., Emori, S., Erda, L., Hibbard, K., et al., 2008. *Towards New Scenarios for the Analysis of Emissions: Climate Change, Impacts and Response Strategies*. Intergovernmental Panel on Climate Change Secretariat (IPCC), Geneva, Switzerland.

[26] Tolman, Hendrik L., 2014. *The WAVEWATCH III Development Group (2014). User Manual and System Documentation of WAVEWATCH III version 4.18, Tech. Note 316*. NOAA/NWS/NCEP/MMAB, Washington, DC. See also URL http://polar.ncep.noaa.gov/waves/wavewatch/manual.v4.18.pdf.

[27] Gallagher, Sarah and Gleeson, Emily and Tiron, Roxana and McGrath, Ray and Dias, Frédéric, 2016. "Twenty-First Century Wave Climate Projections for Ireland and Surface Winds in the North Atlantic Ocean". *Advances in Science and Research,* ***13***, pp. 75–80.

[28] Hurrell, James and National Center for Atmospheric Research Staff, 2003. *The Climate Data Guide: Hurrell North Atlantic Oscillation (NAO) Index (station-based)*. Last modified 07 Jul 2017. Retrieved from https://climatedataguide.ucar.edu/climate-data/hurrell-north-atlantic-oscillation-nao-index-station-based.

[29] Schulzweida, Uwea and Kornblueh, Luis and Quast Ralf, 2006. *CDO users guide*. Climate Data Operators, Version 1 no. 6.

[30] Janjić, J., Gallagher, S., Gleeson, E., and Dias, F., 2017. "Wave energy potential in the northeast Atlantic: Impact of large-scale atmospheric oscillations". In 1st Workshop on Waves, Storm Surges and Coastal Hazards, pp. 1–5. P26.

[31] Janjić, J., Gallagher, S., and Dias, F., 2017. "The Future Northeast Atlantic Wave Energy Potential under Climate Change". In Proceedings of the 27th International Ocean and Polar Engineering Conference ISOPE, San Francisco, CA, USA, June 25-30, 2017, pp. 199–206. ISBN 978-1-880653-97-5; ISSN 1098-6189.

[32] Janjić, J., Gallagher, S., and Dias, F., 2017. "Wave Energy Extraction in the Northeast Atlantic: Future Wave Climate Availability". In Proceedings of the 12th European Wave and Tidal Energy Conference EWTEC, 27th Aug – 1st Sept 2017, Cork, Ireland, pp. 870:1–9. ISSN 2309-1983.